Experimental Validation of a Lithium-Ion Battery State of Charge Estimation with an Extended Kalman Filter

Carmelo Speltino, Domenico Di Domenico, Giovanni Fiengo and Anna Stefanopoulou

***Abstract*— In this paper an averaged electrochemical lithium-ion battery model, presented and discussed in [2] and [3], is identified and validated through experimental data by a 10 Ah li-ion battery pack, during charge and discharge experiments.**

The model is based on an approximation relationship between the averaged Butler-Volmer current and the average solid concentration (in positive and negative electrode) at the interface with the electrolyte phase.

The resulting cell-averaged solid diffusion model is then discretized along the radial direction resulting in two sets (negative and positive electrode) of ordinary differential equations. The behavior of the average concentration of the negative electrode is then expressed algebraically with the average positive electrode concentration through the cell SOC. This last model simplification avoids unobservable conditions as discussed in [3] and allow the application of an extended Kalman Filter (EKF) from the measured cell voltage.

The battery State Of Charge (SOC) is then estimated using a 4th order Extended Kalman Filter (EKF) based on the averaged model and the performance is shown experimentally in a 10 cell 37 V at 10 Ah Li-ion battery..

Keywords: Battery model, parameter identification, Kalman filter, SOC estimation.

I. Introduction

Lithium-ion batteries play an important role in the area of hybrid vehicle design, scale-up, optimization and control issues of Hybrid-Electrical Vehicles (HEV) as high-rate transient power source. When the batteries operate in a relative limited range of state of charge, high efficiency, slow aging and no damaging are expected. As consequence, the State Of Charge (SOC) estimation and regulation is one of the most important and challenging tasks for hybrid and electrical vehicle control.

Several techniques have been proposed for SOC estimation, like model based observers or black-box methods (as an example using fuzzy-logic [10]). The accuracy reached is about 2% [8]. In order to improve this accuracy, SOC estimation based on electrochemical [4], [14], [17] is investigated. These models are generally preferred to the equivalent circuit, or to other kinds of simplified models, thanks to their ability to predict the physical cells limitations, which have a relevant effect in the automotive application, where the battery suffers very often the stress of very high transient loads [12].

Carmelo Speltino, Domenico Di Domenico and Giovanni Fiengo are with Dipartimento di Ingegneria, Università degli Studi del Sannio, Piazza Roma 21, 82100 Benevento. E-mail: {carmelo.speltino, domenico.didomenico, gifiengo}@unisannio.it

Anna Stefanopoulou is with Mechanical Engineering Univ of Michigan, Ann Arbor MI 48109-2121. E-mail: annastef@umich.edu.

Unfortunately, the high order of electrochemical model and the complexity make a real-time on-board estimator difficult to realize. As a consequence several approximations are typically introduced [1], [7].

To this aim, the authors of the present work have proposed in previous paper (see [2] and [3]) an average electrochemical model suitable for a feasible solid concentration estimation. The model is based on an approximated relationship between (i) the Butler-Volmer current and the solid concentration at the interface with the electrolyte and (ii) the battery current and voltage. It shows a maximum error of 0.3 mV on the predicted cell voltage when it is compared with a full order electrochemical model. Based on this simplified model a 4th order extended Kalman filter (EKF) is also designed for SOC estimation.

In this work, the averaged model parameters are identified in order to match the model output with the experimental data. The model is then validated using battery voltage and current measurements during both charge and discharge experiments. Finally the extended Kalman filter parameters are adjusted in order to estimate the battery solid concentration and, as consequence, the battery SOC.

The paper is organized as follows. Firstly, the electrochemical model is briefly described. Then the experimental set-up and the battery parameters identification procedure are illustrated. The extended Kalman filter features and SOC estimation are finally presented in section IV and V.

II. Electrochemical battery model

The battery is composed of three main parts: the negative electrode, the separator and the positive electrode. Referring to a battery with porous electrode material, each electrode consists of a solid matrix inside an electrolyte solution, while the separator is just the electrolyte solution. In particular, for the Lithium-ion battery, the negative electrode, or anode, is generally composed of carbon, while the positive electrode, or cathode, is a metal oxide and the electrolyte is a lithium salt in an organic solvent, such as $LiPF_6$.

The separator is a solid or liquid solution with high concentration of lithium ion. It conducts the ion but it is an electronic insulator. At the negative electrode, the solid active material particles of lithium (Li_xC_6) diffuse to the electrolyte-solid interface where the chemical reaction occurs, transferring the lithium ions to the solution and the electrons to the collector [12]. The produced lithium ions flow through the solution to the positive electrode, where, at the interface with solid material, they react again with

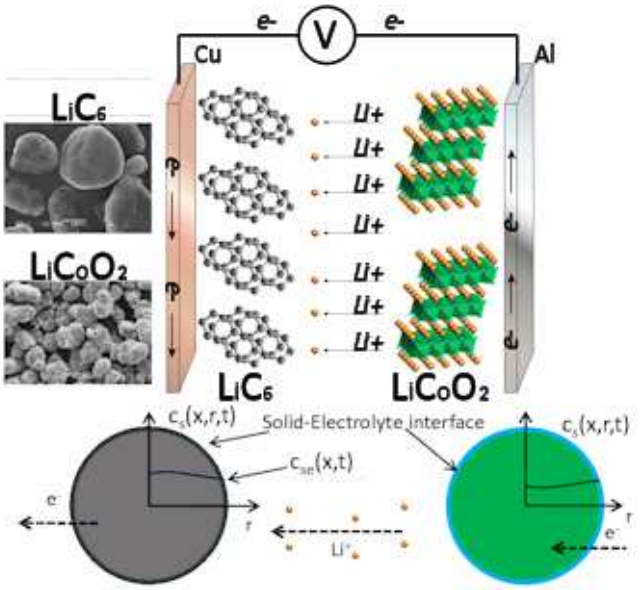

Fig. 1. Schematic macroscopic (x-direction) cell model with coupled microscopic (r-direction) solid diffusion model.

electron coming from positive collector and insert into the metal oxide solid particles.

It's generally accepted that a microscopic description of the battery is intractable, due to the complexity of the phenomena at the interfaces [15]. So, in order to mathematically model the battery, both macroscopic and microscopic modeling approximations have to be considered.

The equations used in this paper describe the battery system with four quantities, i.e. solid and electrolyte concentrations (c_s, c_e) and solid and electrolyte potentials (ϕ_s, ϕ_e)(see [5], [12]).

$$\frac{\partial}{\partial x}\left(\kappa^{eff}\overrightarrow{\nabla}_x\phi_e + \kappa_D^{eff}\overrightarrow{\nabla}_x \ln c_e\right) = -j^{Li} \tag{1}$$

$$\frac{\partial}{\partial x}\left(\sigma^{eff}\overrightarrow{\nabla}_x\phi_s\right) = j^{Li} \tag{2}$$

$$\frac{\partial \epsilon_e c_e}{\partial t} = \overrightarrow{\nabla}_x\left(D_e^{eff}\overrightarrow{\nabla}_x c_e\right) + \frac{1-t^0}{F}j^{Li} \tag{3}$$

$$\frac{\partial c_s}{\partial t} = \overrightarrow{\nabla}_r(D_s\overrightarrow{\nabla}c_s) \tag{4}$$

coupled with the Butler-Volmer current density equation

$$j^{Li}(x) = a_s j_0\left[\exp\left(\frac{\alpha_a F}{RT}\eta\right) - \exp\left(-\frac{\alpha_c F}{RT}\eta\right)\right] \tag{5}$$

where the overpotential η is obtained as

$$\eta = \phi_s - \phi_e - U(c_{se}) \tag{6}$$

where $U(c_{se})$ is the open circuit potential which is an empirical correlation function of the solid concentrations and the coefficient j_0 calculated as

$$j_0 = k_0(c_e)^{\alpha_a}(c_{s,max} - c_{se})^{\alpha_a}(c_{se})^{\alpha_c}. \tag{7}$$

The cell potential is computed as

$$V = \phi_s(x=L) - \phi_s(x=0) - \frac{R_f}{A}I \tag{8}$$

where R_f is the film resistance on the electrodes surface and A is the collectors surface. More details on the model and its parameters can be found in [2], [12], [16].

A model simplification can be achieved by neglecting the solid concentration distribution along the electrode and considering the material diffusion inside a representative solid material particle for each electrode. This simplification introduces an average value for the solid concentration which can be related with the definition of battery state of charge. Furthermore, by assuming high concentration of electrolyte material in the solution, the electrolyte concentration c_e can be considered constant and its average value can be used in the model.

Although these simplifications result in a heavy loss of information, they can be useful in control and estimation applications as we demonstrate next. In accordance with the mean solid concentration, the spatial dependence of the Butler-Volmer current is ignored and a constant value $\bar{j}^{Li}$ is considered which satisfies the spacial integral (for the anode or the cathode)

$$\int_0^{\delta_n} j^{Li}(x)dx = \frac{I}{A} = \bar{j}_n^{Li}\delta_n \tag{9}$$

where δ_n is the anode thickness. This averaging procedure is equivalent to considering a representative solid material particle somewhere along the anode and the cathode [3].

The partial differential equation (4), describes the solid phase concentration along the radius of active particle, but the macroscopic model requires only the concentration at the electrolyte interface.

By using the finite difference method for the spatial variable r, it is possible to express the spherical PDE into a set of ordinary differential equations (ODE), dividing the sphere radius in $M_r - 1$ slices, each of size $\Delta_r = \frac{R_s}{M_r - 1}$ and rewriting boundary conditions [11]. The new system presents $M_r - 1$ states $\mathbf{c_s} = (c_{s_1}, c_{s_2}, ...c_{s_{M_r-1}})^T$, representing radially distributed concentrations at finite element node points $1, ..., M_r - 1$

$$\dot{c}_s = \mathbf{A}c_s + \mathbf{B}\bar{j}^{Li}. \tag{10}$$

where $\mathbf{A}$ is a constant tri-diagonal matrix, function of the diffusion coefficient D_s. The output of the system is the value of the solid concentration at the sphere radius, that can be rewritten as

$$\bar{c}_{se} = c_{s_{M_r-1}} - \mathbf{D}\bar{j}^{Li}. \tag{11}$$

where $\mathbf{D}$ is function of diffusion coefficient D_s and active surface area a_s. Two sets of ODEs, one for the anode and one for the cathode are then obtained. The positive and negative electrode dynamical systems differ at the constant values and at the input sign.

The initial values of $\bar{c}_{se}$ when the battery is fully charged is defined as $\bar{c}_{se,x}^{100\%}$ and when fully discharged as $\bar{c}_{se,x}^{0\%}$,

with $x = p, n$ for the positive and negative electrode. It is convenient to define the normalized concentration, also know as stoichiometry, $\theta_x = \bar{c}_{se,x}/c_{se,max,x}$, with $x = p, n$ for the positive and negative electrode.

The battery voltage (8), using (6) and using the average values at the anode and the cathode, can be rewritten as

$$\begin{aligned} V(t) = (\bar{\eta}_p - \bar{\eta}_n) + \left(\bar{\phi}_{e,p} - \bar{\phi}_{e,n}\right) \\ + (U_p(\theta_p) - U_n(\theta_n)) - \frac{R_f}{A} I. \end{aligned} \tag{12}$$

Using the microscopic current average values and imposing the boundary conditions and the continuity at the interfaces, a solution of equations (1) - (4) can be found. The results can be found in [2] and [3] and are not reported here for brevity. Further simplification is however, required to arrive to a computationally-tractable and observable model as discussed below.

Using (5) it is possible to express the overpotentials difference as function of average current densities and solid concentrations as follows

$$\bar{\eta}_p - \bar{\eta}_n = \frac{RT}{\alpha_a F} \ln \frac{\xi_p + \sqrt{\xi_p^2 + 1}}{\xi_n + \sqrt{\xi_n^2 + 1}} \tag{13}$$

where

$$\xi_p = \frac{\bar{j}_p^{Li}}{2 a_s j_{0p}} \quad \text{and} \quad \xi_n = \frac{\bar{j}_n^{Li}}{2 a_s j_{0n}}. \tag{14}$$

The approximate solution for the electrolyte potential at the interface with the collectors leads to

$$\bar{\phi}_{e,p} - \bar{\phi}_{e,n} = \phi_e(L) - \phi_e(0) = -\frac{I}{2Ak^{eff}} \left(\delta_n + 2\delta_{sep} + \delta_p\right). \tag{15}$$

Finally, the battery voltage (12) can be rewritten as a function of current demand and average solid concentration

$$\begin{aligned} V(t) = \frac{RT}{\alpha_a F} \ln \frac{\xi_p + \sqrt{\xi_p^2 + 1}}{\xi_n + \sqrt{\xi_n^2 + 1}} \\ + (U_p(\theta_p) - U_n(\theta_n)) - \frac{K_r}{A} I. \end{aligned} \tag{16}$$

where $K_r = \frac{1}{2Ak^{eff}} \left(\delta_n + 2\delta_{sep} + \delta_p\right) + R_f$ is a term that takes into account both internal and collector film resistances.

III. Model Parameter Identification and Validation

The battery adopted for the experiments is a Powerizer - Polymer $Li - Ion$ Battery Pack, composed of 10 cells. Its nominal voltage is 37 V at 10 Ah. The battery has been charged and discharged using the electronic load Prodigit 3260, coupled with a DC generator. The data has been collected using an ADC of the National Instrument, able to sample multiple channels up to 1 MHz with 16 bit of precision.

In order to acquire experimental data to identify the model parameters and test the SOC estimator, several charges and discharges of the battery have been performed and the coupled voltage and current data sets have been collected. Then an identification procedure, based on gradient free function minimization algorithm, has been designed in order to estimate the parameters values that best fit the output of the averaged model versus all the collected data. The parameters to identify are the maximum positive and negative solid concentration $c_{s,max,p}$ and $c_{s,max,n}$, the positive and negative solid phase diffusion coefficient $D_{s,p}$ and $D_{s,n}$, the positive and negative active surface area per electrode $a_{s,p}$ and $a_{s,n}$, the electrode surface A, the total cell film resistance K_r and the current coefficient k_0 for a total of nine parameters.

Figures 2 reports the performance of the averaged model versus the battery output during an identification test. The experiment corresponds to a power request profile, simulating a variable load connected to the battery. It shows a good battery voltage prediction, with a maximum absolute error of 0.2 V. The bottom subplot of Figure 2 shows the voltage error. Even if the error exhibits a high value during transients, a good performance during constant current operation can be noticed.

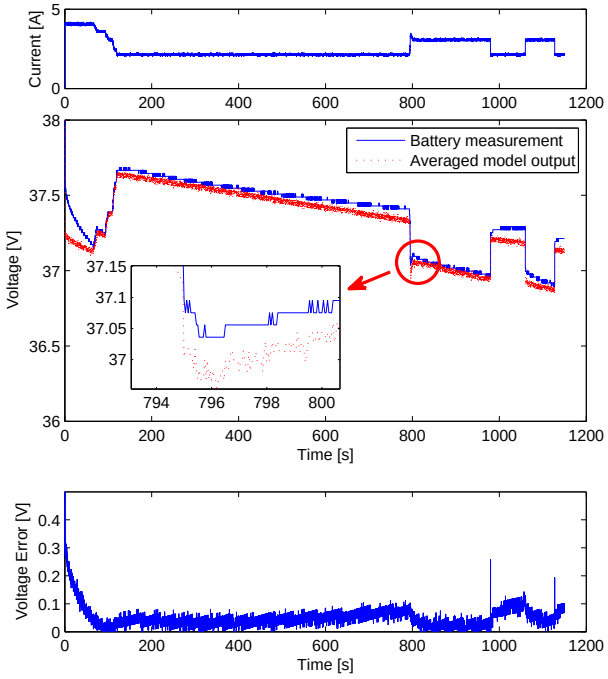

Fig. 2. Averaged model versus experimental data: requested current; measured (solid-blue line) and simulated (dotted-red line)battery voltage; voltage error.

Finally, Tables I and II show the battery constants and the identified parameters, respectively. Detail of the identification process and the identification results are discussed in [13].

IV. Kalman filter State of Charge estimation

The physical quantity related to the battery state of charge is the solid concentration at the electrodes. A Kalman Filter for the on-line SOC estimation based on the electrochemical model is presented in [2], where a preliminary observability analysis is also performed.

Parameter	Negative electrode	Separator	Positive electrode
Thickness (cm)	$\delta_n = 50 \times 10^{-4}$	$\delta_{sep} = 25.4 \times 10^{-4}$	$\delta_p = 36.4 \times 10^{-4}$
Particle radius R_s (cm)	1×10^{-4}	-	1×10^{-4}
Active material volume fraction ε_s	0.580	-	0.500
Electrolyte phase volume fraction (porosity) ε_e	0.332	0.5	0.330
Conductivity of solid active material σ ($\Omega^{-1}\ cm^{-1}$)	1	-	0.1
Effective conductivity of solid active material	$\sigma^{eff} = \varepsilon_s \sigma$	-	$\sigma^{eff} = \varepsilon_s \sigma$
Transference number t_+^0	0.363	0.363	0.363
Electrolyte phase ionic conductivity κ ($\Omega^{-1}\ cm^{-1}$)	$\kappa = 0.0158 c_e \exp(0.85 c_e^{1.4})$	$\kappa = 0.0158 c_e \exp(0.85 c_e^{1.4})$	$\kappa = 0.0158 c_e \exp(0.85 c_e^{1.4})$
Effective electrolyte phase ionic conductivity	$\kappa^{eff} = (\varepsilon_e)^{1.5}\kappa$	$\kappa^{eff} = (\varepsilon_e)^{1.5}\kappa$	$\kappa^{eff} = (\varepsilon_e)^{1.5}\kappa$
Effective electrolyte phase diffusion conductivity	$\kappa_D^{eff} = \frac{2RT\kappa^{eff}}{F}(t_+^0 - 1)$	$\kappa_D^{eff} = \frac{2RT\kappa^{eff}}{F}(t_+^0 - 1)$	$\kappa_D^{eff} = \frac{2RT\kappa^{eff}}{F}(t_+^0 - 1)$
Electrolyte phase diffusion coefficient D_e ($cm^2\ s^{-1}$)	2.6×10^{-6}	2.6×10^{-6}	2.6×10^{-6}
Effective electrolyte phase diffusion coefficient	$D_e^{eff} = (\varepsilon_e)^{1.5} D_e$	$D_e^{eff} = (\varepsilon_e)^{1.5} D_e$	$D_e^{eff} = (\varepsilon_e)^{1.5} D_e$
Change transfers coefficients α_a, α_c	0.5,0.5	-	0.5, 0.5

TABLE I
BATTERY CONSTANT VALUES.

Specifically, the average dynamical system describes the diffusion effects into two solid material particles, one for the cathode and one for the anode, and allows to compute the solid concentration at the spheres radius, which represents an average value of the solid concentration throughout the electrodes. However the cell voltage (33) depends on $(U_p(\theta_p) - U_n(\theta_n))$ making the difference of the open circuit voltage, but not the individual electrode concentrations, observable. Indeed, it was shown in [3] that the system that includes both positive and negative electrode concentration states is weakly observable.

This limitation can be mitigated by establishing a relation between the anode and the cathode average solid concentrations which can be used for the estimation of the negative electrode concentration based on the positive electrode, which can now be observable from the output cell voltage [2].

First, let us define the state of charge of the battery, with a good approximation, as linearly varying with θ between the two reference values at 0% and 100%

$$SOC(t) = \frac{\theta_x - \theta_x^{0\%}}{\theta_x^{100\%} - \theta_x^{0\%}}. \tag{17}$$

with $x = p, n$ for the positive and negative electrode.

Finally, equation (17) allows the computation of negative stoichiometry from positive using (17) as

$$\theta_n = \left(\theta_p - \theta_p^{0\%}\right) \left[\frac{\theta_n^{100\%} - \theta_n^{0\%}}{\theta_p^{100\%} - \theta_p^{0\%}}\right] - \theta_n^{0\%} \tag{18}$$

Hence, introducing the state vector $x = (\bar{c}_{s,p1}, \bar{c}_{s,p2}, ..., \bar{c}_{s,p(M_r-1)})^T$, the dynamical system is

$$\dot{x} = A_p x(t) + B_p u(t), \tag{19}$$

where the input is the average value of the Butler-Volmer current

$$u = \bar{j}_p^{Li} \tag{20}$$

and the output is the measurement of the battery voltage

$$y = V(x, u) \tag{21}$$

function of solid concentration and battery current. The matrices A_p and B_p are obtained from (10). For a linear state-space formulation, the linearized battery voltage results in an output matrix $C = \partial V / \partial x$ which is a row matrix with zeros in its first $M_r - 2$ elements and the last non-zero term equal to

$$\frac{\partial V}{\partial \bar{c}_{s,p(M_r-1)}} = \frac{\partial U_p}{\partial \bar{c}_{s,p(M_r-1)}} - \frac{\partial U_n}{\partial \bar{c}_{se,n}} \frac{\partial \bar{c}_{se,n}}{\partial \bar{c}_{s,p(M_r-1)}}. \tag{22}$$

This guarantees a strongly local observability $\forall \bar{c}_{se,p} \neq 0$ [2], [6], [9].

The Kalman filter can now be designed, according to

$$\begin{aligned} \dot{\hat{x}} &= A_p \hat{x} + Bu + K_e(y - \hat{y}) \\ \hat{y} &= V(\hat{x}, u) \end{aligned} \tag{23}$$

where $\hat{x}$ and $\hat{y}$ are respectively the estimate state and output, V is the output nonlinear function in (16), A_p, B_p are the matrices describing the dynamical system introduced by (19), C defined using (22) and K_e is the Kalman gain, obtained as follows

$$K_e = PCR_u^{-1} \tag{24}$$

where P is the solution of the Riccati equation

$$\begin{aligned} \dot{P} &= A_p P + PA_p^T - PCR_u^{-1}C^T P + R_x \\ P(0) &= P_0, \end{aligned} \tag{25}$$

and R_x and R_u are weight matrices appropriately tuned in order to minimize the quadratic error on battery voltage. A Matlab optimization procedure returned $R_x = 10 \times \mathbf{I}$ (where $\mathbf{I}$ is the identity matrix) and $R_u = 12$.

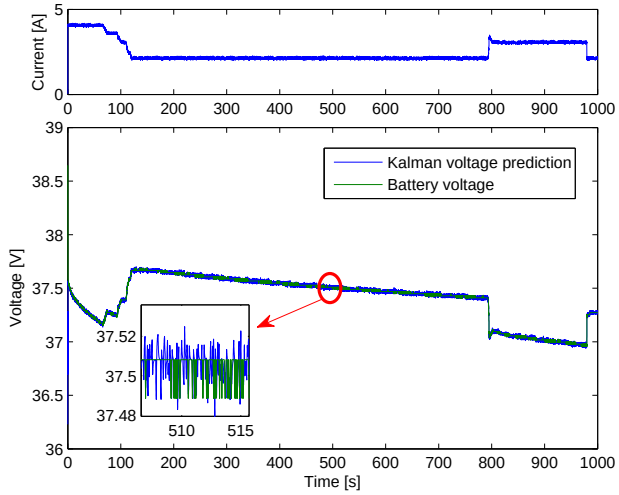

Fig. 3. Experiment 1: current and voltage experimental data during a battery discharge. The battery voltage measurement (dotted-green line) is compared with the output filter estimation (solid-blue line).

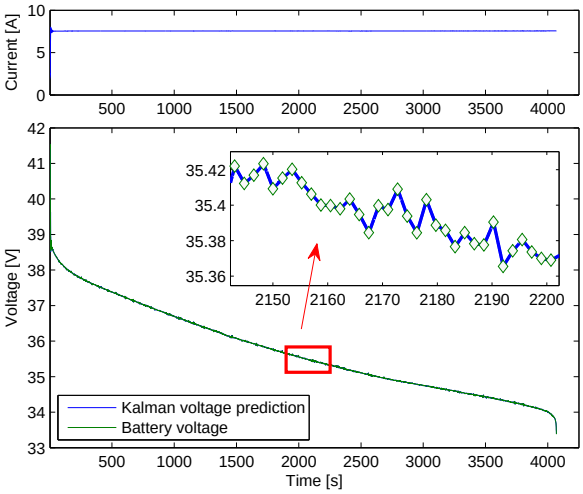

Fig. 5. Experiment 2: current and voltage experimental data during a full discharge. The battery voltage measurement (dotted-green line) is compared with the filter estimation (solid-blue line).

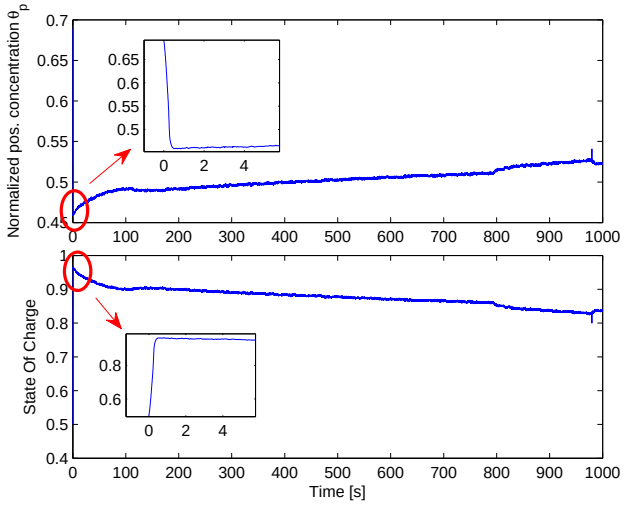

Fig. 4. Experiment 1: solid concentration and SOC estimation.

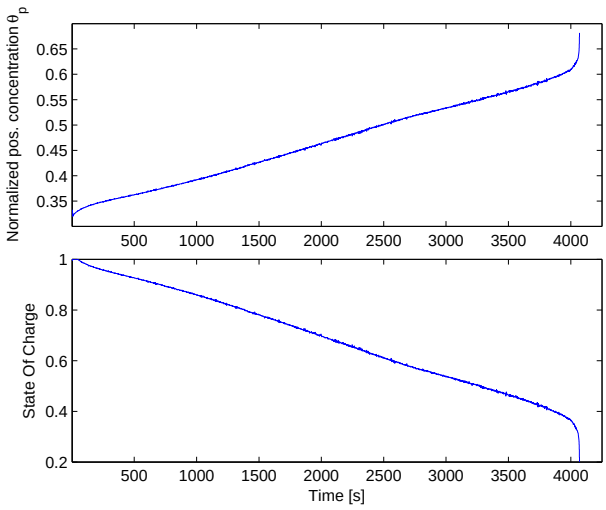

Fig. 6. Experiment 2: solid concentration and SOC estimation.

V. Experimental results

In this section the simulation results compared to the experimental data are reported, in order to demonstrate the performance of the Kalman filter. The experiments are similar to the ones used validate the model.

Figures 3 - 6 show the filter performance during two selected experiments and its very fast recovery of the voltage error thanks to feedback regulation. In the first, starting from the battery almost fully charged, a variable load is applied (see the first plot of Figure 3) and the battery is discharged for about 1000 s. The output voltage is correctly estimated, as it is possible to note in the second plot of Figure 3, where it is compared with the experimental data. The estimated SOC is shown in Figure 4 to decrease by 10%, consistently with the discharge rates (mostly 0.3 C) and the discharge duration (1000 s). The second set of experiments is a nearly complete battery discharge with constant current load (about 7.5 A), starting from 100% SOC. Again the battery voltage is optimally estimated (see the comparison with the experimental data shown in the second plot of Figure 5) and SOC estimation (shown in Figure 6), which almost reaches the minimum value. The SOC estimation exhibits the expected behavior, in coherence with simple coloumb counting. The voltage error is almost zero again thanks to the great error recovery property of the Kalman filter.

Finally a robustness analysis has been performed on the Kalman filter to verify the robustness of the observer to variation of the model parameters. The results of this analysis are listed in Table III showing excellent performance in terms of robustness and reliability with respect to the variation of

Name	Symbol and Value
Max negative solid concentration *(mol cm^{-3})*	$c_{s,max,p} = 1.119 \times 10^{-2}$
Max positive solid concentration *(mol cm^{-3})*	$c_{s,max,p} = 4.568 \times 10^{-2}$
Average solid concentration *(mol cm^{-3})*	$\bar{c}_e = 7.556 \times 10^{-4}$
Solid phase neg. diffusion coefficient *($cm^2\ s^{-1}$)*	$D_{s,n} = 2.32 \times 10^{-12}$
Solid phase pos. diffusion coefficient *($cm^2\ s^{-1}$)*	$D_{s,p} = 3.95 \times 10^{-12}$
Negative active surface area per electrode ($cm^2 cm^{-3}$)	$a_{s,n} = 1.71 \times 10^4$
Positive active surface area per electrode ($cm^2 cm^{-3}$)	$a_{s,p} = 2.07 \times 10^4$
Electrode plate Area cm^2	$A = 10166$
Total resistance (internal and external) Ωcm^2	$K_r = 258.456$
Current density coefficient	$k_0 = 1.124 \times 10^3$

TABLE II

IDENTIFIED PARAMETERS.

one or more model parameters. For brevity the Table III shows just the parameters that lead to a significant SOC estimation variation.

Parameter	Variation	Absolute error mean and std
$cs_{max,p}$	-20%	$\bar{e} = 1.1 \times 10^{-3}$,$s = 3.6 \times 10^{-3}$
	-10%	$\bar{e} = 4.76 \times 10^{-4}$,$s = 1.7 \times 10^{-3}$
	$+10\%$	$\bar{e} = 4.25 \times 10^{-4}$,$s = 1.6 \times 10^{-3}$
	$+20\%$	$\bar{e} = 8.10 \times 10^{-3}$,$s = 3.1 \times 10^{-3}$
$cs_{max,n}$	-20%	$\bar{e} = 2.1 \times 10^{-3}$,$s = 1.8 \times 10^{-4}$
	-10%	$\bar{e} = 9.44 \times 10^{-4}$,$s = 8.02 \times 10^{-5}$
	$+10\%$	$\bar{e} = 7.73 \times 10^{-4}$,$s = 6.57 \times 10^{-5}$
	$+20\%$	$\bar{e} = 1.4 \times 10^{-3}$,$s = 1.2 \times 10^{-4}$
$D_{s,n}$	-20%	$\bar{e} = 7.33 \times 10^{-5}$,$s = 1.73 \times 10^{-4}$
	-10%	$\bar{e} = 3.54 \times 10^{-5}$,$s = 8.71 \times 10^{-5}$
	$+10\%$	$\bar{e} = 3.33 \times 10^{-5}$,$s = 8.8 \times 10^{-5}$
	$+20\%$	$\bar{e} = 6.5 \times 10^{-5}$,$s = 1.76 \times 10^{-4}$
$a_{s,p}$	-20%	$\bar{e} = 5.58 \times 10^{-4}$,$s = 6.7 \times 10^{-5}$
	-10%	$\bar{e} = 2.48 \times 10^{-4}$,$s = 2.97 \times 10^{-5}$
	$+10\%$	$\bar{e} = 2.03 \times 10^{-4}$,$s = 2.43 \times 10^{-5}$
	$+20\%$	$\bar{e} = 3.72 \times 10^{-4}$,$s = 4.47 \times 10^{-5}$
$a_{s,n}$	-20%	$\bar{e} = 2.12 \times 10^{-3}$,$s = 1.8 \times 10^{-4}$
	-10%	$\bar{e} = 9.44 \times 10^{-4}$,$s = 8.03 \times 10^{-5}$
	$+10\%$	$\bar{e} = 7.73 \times 10^{-4}$,$s = 6.57 \times 10^{-5}$
	$+20\%$	$\bar{e} = 1.41 \times 10^{-3}$,$s = 1.2 \times 10^{-4}$
A	-20%	$\bar{e} = 3.57 \times 10^{-3}$,$s = 3.19 \times 10^{-4}$
	-10%	$\bar{e} = 1.6 \times 10^{-3}$,$s = 1.42 \times 10^{-4}$
	$+10\%$	$\bar{e} = 1.3 \times 10^{-3}$,$s = 1.16 \times 10^{-4}$
	$+20\%$	$\bar{e} = 2.39 \times 10^{-3}$,$s = 2.14 \times 10^{-4}$
A and $a_{s,n}$	-20%	$\bar{e} = 2.15 \times 10^{-2}$,$s = 4.66 \times 10^{-3}$
	-10%	$\bar{e} = 1.1 \times 10^{-2}$,$s = 2.45 \times 10^{-3}$
	$+10\%$	$\bar{e} = 1.3 \times 10^{-2}$,$s = 2.11 \times 10^{-3}$
	$+20\%$	$\bar{e} = 2.87 \times 10^{-2}$,$s = 4.31 \times 10^{-3}$

TABLE III

ROBUSTNESS ANALYSIS RESULTS.

VI. CONCLUSION

An isothermal electrochemical model of the Lithium-ion battery was used to derive an averaged model coupling the average microscopic solid material concentration with the average values of the chemical potentials, electrolyte concentration and microscopic current density. The average model was identified using a 10 Ah battery pack experimental data. Finally, the SOC estimation was performed using an EKF, showing excellent results in term of voltage convergence indicating good and fast battery SOC estimation and robustness to widely battery parameters variations.

REFERENCES

[1] O. Barbarisi, F. Vasca, and L. Glielmo. State of charge kalman filter estimator for automotive batteries. *Control Engineering Practice*, 14:267 – 275, 2006.

[2] D. Di Domenico, G. Fiengo, and A. Stefanopoulou. Lithium-ion battery state of charge estimation with a kalman filter based on a electrochemical model. *Proceedings of 2008 IEEE Conference on Control Applications*, 1:702 – 707, 2008.

[3] D. Di Domenico, A. Stefanopoulou, and G. Fiengo. Reduced order lithium-ion battery electrochemical model and extended kalman filter state of charge estimation. *ASME Journal of Dynamic Systems, Measurement and Control - Special Issue on Physical System Modeling*, 2008.

[4] M. Doyle, T.F. Fuller, and J. Newman. Modeling of galvanostatic charge and discharge of the lithium/polymer/insertion cell. *J. Electrochem. Soc.*, 140, 1993.

[5] W.B. Gu and C.Y. Wang. Thermal and electrochemical coupled modeling of a lithium-ion cell. *Proceedings of the ECS*, 99, 2000.

[6] R. Hermann and A. J. Krener. Nonlinear controllability and observability. *IEEE Trans. Aut. Contr.*, pages 728–740, 1977.

[7] B. Paxton and J. Newmann. Modeling of nickel metal hydride. *Journal of Electrochemical Society*, 144, 1997.

[8] V. Pop, H. J. Bergveld, J. Veld, P. Regtien, D. Danilov, and P. Notten. Modeling battery behavior for accurate state-of-charge indication. *J. Electrochem. Soc.*, 153, 2006.

[9] W. Respondek. *Geometry of Static and Dynamic Feedback*. in Mathematical Control Theory, Lectures given at the Summer Schools on Mathematical Control Theory Trieste, Italy, 2001.

[10] A.J. Salkind, C. Fennie, P. Singh, T. Atwater, and D.E. Reisner. Determination of state-of-charge and state-of-health of batts. by fuzzy logic methodology. *J. Power Sources*, 80:293–300, 1999.

[11] W.E. Schiesser. *The Numerical Method of Lines: Integration of Partial Differential Equations*. Elsevier Science & Technology, 1991.

[12] K. Smith and C.Y. Wang. Solid-state diffusion limitations on pulse operation of a lithium-ion cell for hybrid electric vehicles. *Journal of Power Sources*, 161:628–639, 2006.

[13] C. Speltino, D. Di Domenico, A. Stefanopoulou, and G. Fiengo. Experimental identification and validation of an electrochemical model of a lithium-ion battery. *Proceedings of 2009 IEEE European Control Conference*, 2009.

[14] P. De Vidts, J. Delgado, and R.E. White. Mathematical modeling for the discharge of a metal hydride electrode. *J. Electrochem. Soc.*, 142, 1995.

[15] C.Y. Wang, W.B. Gu, and B.Y. Liaw. Micro-macroscopic coupled modeling of batteries and fuel cells. part i: Model development. *J. Electrochem. Soc.*, 145, 1998.

[16] C.Y. Wang, W.B. Gu, and B.Y. Liaw. Micro-macroscopic coupled modeling of batteries and fuel cells. part ii: Application to ni-cd and ni-mh cells. *J. Electrochem. Soc.*, 145, 1998.

[17] J.W. Weidner and P. Timmerman. Effect of proton diffusion, electron conductivity, and charge-transfer resistance on nickel hydroxide discharge curves. *J. Electrochem. Soc.*, 141, 1994.